Am J Physiol Endocrinol Metab 311: E346–E357, 2016.
First published May 31, 2016; doi:10.1152/ajpendo.00045.2016.

Glucose uptake saturation explains glucose kinetics profiles measured by different tests

Roberto Bizzotto,[1] Andrea Natali,[2] Amalia Gastaldelli,[3] Elza Muscelli,[2] Martin Krssak,[4] Attila Brehm,[4] Michael Roden,[5,6,7] Ele Ferrannini,[2,3] and Andrea Mari[1]

[1]*CNR Institute of Neuroscience, Padua, Italy;* [2]*Department of Internal Medicine, University of Pisa School of Medicine, Pisa, Italy;* [3]*CNR Institute of Clinical Physiology, Pisa, Italy;* [4]*Hanusch Hospital, Vienna, Austria;* [5]*Heinrich-Heine University, Düsseldorf, Germany;* [6]*German Diabetes Center, Düsseldorf, Germany; and* [7]*German Center of Diabetes Research, München-Neuherberg, Germany*

Submitted 2 February 2016; accepted in final form 23 May 2016

Bizzotto R, Natali A, Gastaldelli A, Muscelli E, Krssak M, Brehm A, Roden M, Ferrannini E, Mari A. Glucose uptake saturation explains glucose kinetics profiles measured by different tests. *Am J Physiol Endocrinol Metab* 311: E346–E357, 2016. First published May 31, 2016; doi:10.1152/ajpendo.00045.2016.—It is known that for a given insulin level glucose clearance depends on glucose concentration. However, a quantitative representation of the concomitant effects of hyperinsulinemia and hyperglycemia on glucose clearance, necessary to describe heterogeneous tests such as euglycemic and hyperglycemic clamps and oral tests, is lacking. Data from five studies (123 subjects) using a glucose tracer and including all the above tests in normal and diabetic subjects were collected. A mathematical model was developed in which glucose utilization was represented as a Michaelis-Menten function of glucose with constant K_m and insulin-controlled V_{max}, consistently with the basic notions of glucose transport. Individual values for the model parameters were estimated using a population approach. Tracer data were accurately fitted in all tests. The estimated K_m was 3.88 (2.83–5.32) mmol/l [median (interquartile range)]. Median model-derived glucose clearance at 600 pmol/l insulin was reduced from 246 to 158 $ml \cdot min^{-1} \cdot m^{-2}$ when glucose was raised from 5 to 10 mmol/l. The model reproduced the characteristic lack of increase in glucose clearance when moderate hyperinsulinemia was accompanied by hyperglycemia. In all tests, insulin sensitivity was inversely correlated with BMI, as expected ($R^2 = 0.234$, $P = 0.0001$). In conclusion, glucose clearance in euglycemic and hyperglycemic clamps and oral tests can be described with a unifying model, consistent with the notions of glucose transport and able to reproduce the suppression of glucose clearance due to hyperglycemia observed in previous studies. The model may be important for the design of reliable glucose homeostasis simulators.

uptake saturation; glucose metabolism; insulin sensitivity; glucose tracers; mathematical models

THE ACTION OF INSULIN on in vivo glucose kinetics has been subject of extensive studies in the 1970s and 1980s, particularly with the introduction of the glucose clamp technique and glucose tracers. These studies have demonstrated that, at steady state, glucose utilization is a sigmoidal function of insulin concentration. Furthermore, for a given insulin level, glucose utilization does not increase in proportion to glucose concentration: at higher concentrations, utilization is lower than that predicted by a proportional relationship. This implies that at any given insulin concentration glucose clearance, which is the ratio between glucose utilization and concentration, is a decreasing function of glucose concentration. While the glucose clamp conditions have been widely investigated, in dynamic conditions such as oral glucose loading or mixed meal ingestion the impact of the dependency of glucose clearance on glucose concentration is not known. Elucidating this aspect is important for understanding glucose homeostasis. Nevertheless, most of the mathematical models of glucose homeostasis have ignored this phenomenon; in the few models accounting for it [e.g., the model by Dalla Man et al. (11)], its mathematical description has been postulated but not experimentally validated on appropriate data. This limits a full understanding of the control of glucose tolerance and the development of reliable models capable of predicting the outcome of therapeutic interventions.

Exploring the dependency of glucose clearance on glucose concentration is made difficult by the need of complex experimental procedures (44). To overcome this limitation, we sought to exploit the results of several studies testing various and complementary aspects of glucose kinetics and to employ population modeling to interpret all data within a unique framework. The model was based on established notions concerning glucose kinetics and utilization and in particular accounted for saturation of glucose uptake due to the kinetics characteristics of insulin-dependent glucose transport into the cells. Our results indicate that a single model of the relationship between glucose utilization and glucose and insulin concentrations can explain all our experimental observations consistently. We show for the first time that the same physiological mechanisms may underlie different tests such as the clamp, the oral glucose tolerance test (OGTT) and the mixed-meal test (MTT), and we provide a mathematical model capable of describing these phenomena accurately.

MATERIALS AND METHODS

The data used in this analysis were obtained from five different studies of glucose kinetics and insulin action: a three-step hyperglycemic hyperinsulinemic clamp (HGclamp, $n = 8$) (41); a two-step isoglycemic hyperinsulinemic clamp (ISOclamp, $n = 8$) (34); a paired OGTT and euglycemic hyperinsulinemic clamp in the same volunteers (OGTT/clamp, $n = 8$); a MTT ($n = 91$) (16); and a paired MMT and hyperglycemic hyperinsulinemic clamp in the same subjects (MTT/clamp, $n = 8$) (25). Glucose and insulin ranges in the tests were wide (3.3–24.7 mmol/l and 12-10,584 pmol/l, respectively). In all tests, a glucose tracer was used. The subjects' characteristics are reported in Table 1 for each study and for the whole population. Figure 1 shows the mean (±SE) profiles for plasma glucose and insulin concentration during each test. Protocol

Address for reprint requests and other correspondence: R. Bizzotto, IN-CNR, Corso Stati Uniti 4, 35127 Padua, Italy (e-mail: roberto.bizzotto@isib.cnr.it).

Table 1. *Characteristics of the study subjects*

Study*	*N*	Glucose Tolerance†	Sex	Age‡ (yr)	BMI‡ (kg/m^2)
HGclamp	8	NFG	7 M +1 F	39 (37–54)	34.6 (28.1–41.1)
ISOclamp	8	4 NFG + 4 IFG	8 M	44 (36–50)	29.1 (25.1–35.2)
OGTT/clamp	8	6 NGT + 2 IGT	5 M +3 F	37 (34–50)	27.5 (25.2–30.5)
MTT	91	12 NGT + 13 IGT + 66 T2D	63 M +28 F	60 (50–65)	32.4 (28.8–35.2)
MTT/clamp	8	4 NGT + 4 T2D	5 M +3 F	50 (45–58)	26.2 (24.1–27.9)
All	123	34 NGR + 19 IGR + 70 T2D	88 M +35 F	56 (48–63)	31.6 (27.7–35.0)

M, males; F, females; BMI, body mass index. *See MATERIALS AND METHODS for abbreviations. †ADA 1997 criteria: NFG, normal fasting glucose; IFG, impaired fasting glucose; NGT, normal glucose tolerance; IGT, impaired glucose tolerance; T2D, type 2 diabetes; NGR, normal glucose regulation (see MATERIALS AND METHODS); IGR, impaired glucose regulation (see MATERIALS AND METHODS). ‡Median (interquartile range).

details and analytic procedures are provided in APPENDIX A. All studies have been approved by local or Institutional Ethics Committees, and informed consents were obtained from the participants.

Model of glucose kinetics. Glucose kinetics was represented through a circulatory model (27, 28, 32). In the model, a heart-lung block is interconnected with a periphery block lumping all the remaining tissues (Fig. 2). Glucose uptake was considered negligible in the heart-lung block and was modeled as a function of insulin and glucose concentration in the periphery block. A detailed description of the circulatory model is provided in APPENDIX B.

Model of glucose uptake. The transport-mediated rate of glucose uptake in the peripheral tissues, $\varphi(t)$, was represented as a Michaelis-Menten function of glucose concentration at the site of transport, $X(t)$:

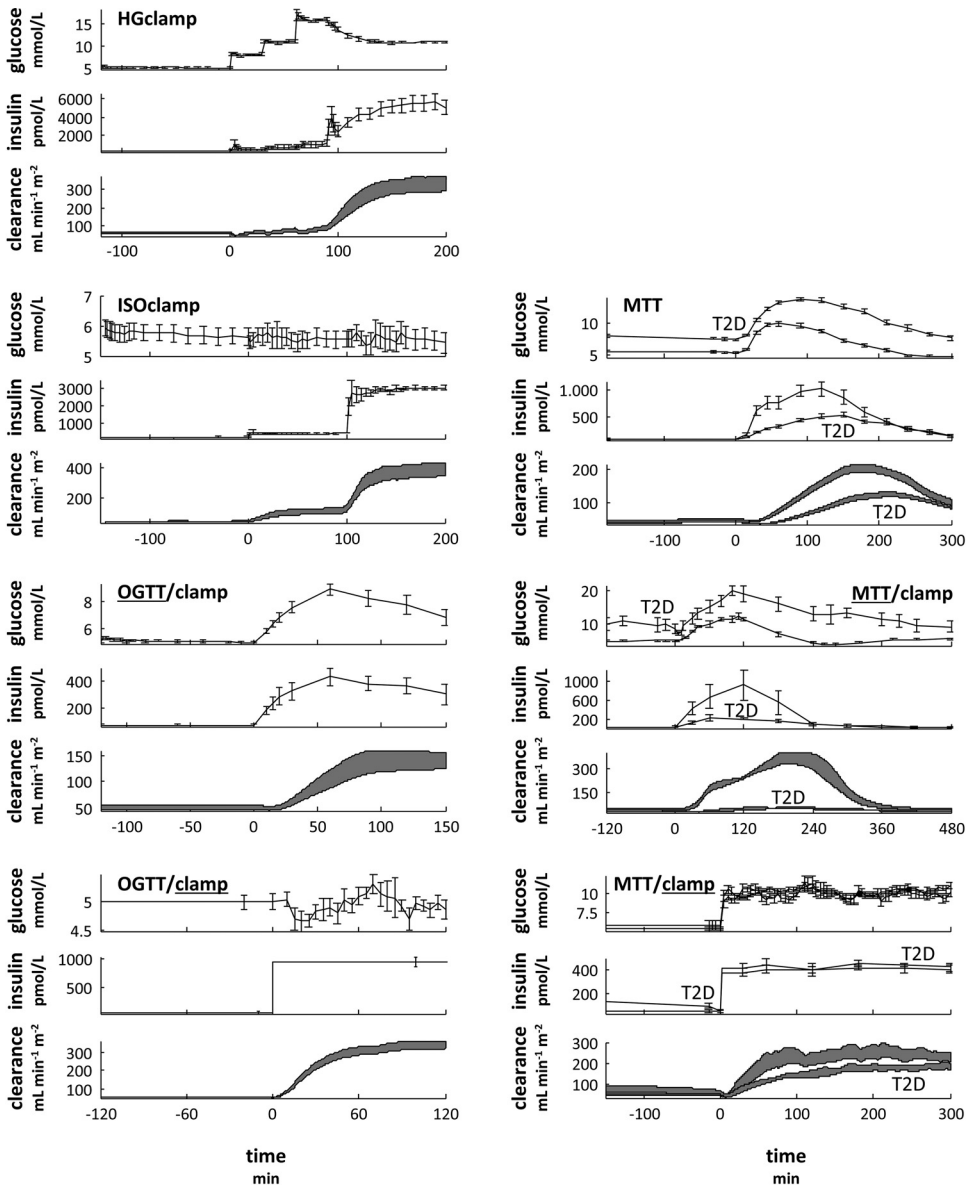

Fig. 1. Mean (±SE as error bars or gray areas) measured plasma glucose and insulin concentrations and model-predicted glucose clearance in the 5 studies, as shown in the figure labels (see MATERIALS AND METHODS for abbreviations). Data were partially published previously (41, 34, 16, 25); see APPENDIX A for details. The data of the 2 studies with paired tests (OGTT/clamp and MTT/clamp) are shown in separate panels for the oral test and the clamp, as indicated by the underlined text in the figure label. The data of the two studies with both diabetic (T2D) and nondiabetic (ND) subjects (MTT and MTT/clamp) are shown with separate profiles for the T2D and ND groups.

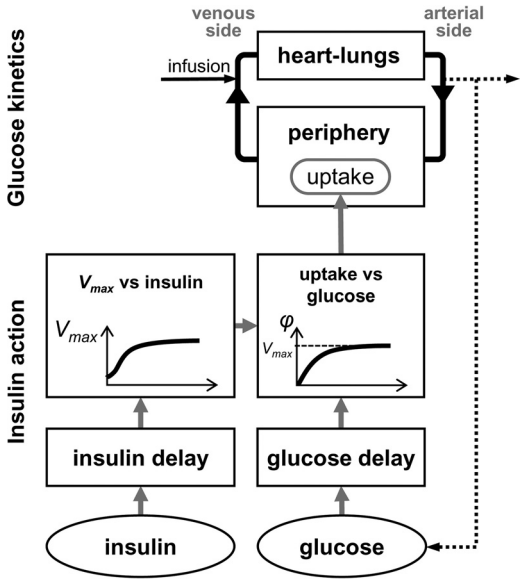

Fig. 2. Model of glucose kinetics and insulin action. Glucose kinetics is described using a circulatory model. Glucose uptake is a Michaelis-Menten function of glucose concentration. Insulin action is exerted on the maximal glucose uptake (V_{max}) through a Hill function of insulin concentration. Both glucose and insulin at the site of action are delayed with respect to plasma concentrations.

$$\varphi(t) = \frac{V_{max}(t)X(t)}{K_{mG} + X(t)} \quad (1)$$

where $V_{max}(t)$ and K_{mG} are the Michaelis-Menten parameters. This function yields a gradual saturation of glucose utilization as glucose levels increase, as expected for glucose transport. K_{mG} was considered to be constant, while $V_{max}(t)$ was assumed to be a function of insulin concentration at the site of action, $Z(t)$, according to a Hill equation:

$$V_{max}(t) = V_{max,0} + \frac{E_{max}Z(t)^{\gamma}}{K_{ml}{}^{\gamma} + Z(t)^{\gamma}} \quad (2)$$

where $V_{max,0}$ is the maximal glucose uptake at zero insulin at the site of action, and E_{max}, K_{mI}, and γ are the Hill function parameters.

Glucose and insulin concentrations at the site of action were described as delayed plasma glucose and insulin concentrations, respectively. Each delayed concentration was computed through a transit compartment model with two compartments (equations in APPENDIX B), i.e., through the series of two monoexponential delays with the same half-lives ($t_{1/2,G}$ and $t_{1/2,I}$, respectively).

Glucose clearance, $cl(t)$, was defined as the ratio between glucose uptake, $\varphi(t)$, and glucose concentration at the site of action, $X(t)$:

$$cl(t) = \frac{V_{max}(t)}{K_{mG} + X(t)}. \quad (3)$$

Distributions of individual parameters. For each model parameter, the individual value was assumed to derive from a probability distribution over the population, as required by the population approach adopted for parameters estimation. The distributions were assumed to be lognormal for the parameters K_{mG}, E_{max}, K_{mI}, γ, and $t_{1/2,I}$ and for the glucose volume of distribution V. Logit distributions in the interval from zero to one were assumed for the individual parameters of the circulatory model that are constrained in this range. A unique value of $V_{max,0}$ was assumed in the whole population (see below); $t_{1/2,G}$ was empirically fixed to 0.7 min, as the model was almost insensitive to moderate changes of its value. In order to reach convergence during parameter estimation, the values for the parameters of the circulatory model estimated in the subjects from the MTT/clamp study had to be constrained to the medians of the probability distributions. Finally, in the OGTT/clamp and MTT/clamp studies, the individual parameter values were assumed to be the same in the two tests.

Parameters estimation and model development. The whole model, comprehensive of the description of the probability distributions for the individual parameters, was implemented using the Monolix software, version 4.3.2 (26). Parameters were estimated by fitting the model to glucose tracer concentrations from all tests and subjects. Measured glucose and insulin concentrations were linearly interpolated and used as inputs of the model. The adopted population (or mixed-effect) approach first identifies the medians (called "typical values") and variances of the parameter distributions according to the maximum likelihood approach. Thereafter, the identified distributions are used as priors to determine maximum a posteriori estimates of the individual parameter values.

Different variants of the model were tested with the objective of reducing the likelihood of the data, i.e., simultaneously improving the data fit and minimizing the variances of the parameter distributions and the number of model parameters. In particular, the investigation focused on different parameterizations of the model equations, on different descriptions of insulin action (Eq. 2), and on the correlations between the parameter distributions. Moreover, we found that the variability of $V_{max,0}$ collapsed to zero, and thus a unique value for all the subjects was used.

Glucose tolerance and insulin sensitivity estimates. The participants were divided into three glucose tolerance classes according to the ADA 1997 criteria: type 2 diabetes (T2D) patients, subjects with either impaired glucose tolerance or impaired fasting glucose (i.e., impaired glucose regulation, IGR), and subjects with none of the previous impairments (i.e., normal glucose regulation, NGR). The last category was used for subjects with normal glucose tolerance (NGT) and for those in whom 2-h glucose was not available but fasting glucose was normal. Insulin sensitivity was computed as the glucose clearance at a steady-state glucose concentration of 5 mmol/l and two insulin concentrations representing the typical concentration of a euglycemic clamp (600 pmol/l) and the mean basal insulin in the NGR subjects of this analysis (71 pmol/l). These two insulin sensitivity indexes were derived in each subject from the individual parameter estimates and denoted as IS_{clamp} and IS_b, respectively.

Assessment of the role of body mass index and study. The individual body mass index (BMI) and the study were investigated as possible statistically significant covariates/factors explaining the variability of insulin sensitivity and of the individual values of the model parameters. *N*-way analysis of variance (ANOVA) was used for this purpose, after logarithmic transformation of the involved variables, and after adjusting for the glucose tolerance status, and for age and sex when significant.

Impact of uptake saturation on glucose levels. A prototypical glucose homeostasis model was implemented for assessing the impact on glucose tolerance of using a saturable function for glucose uptake (Eq. 1) compared with a linear one. The model included the glucose kinetics model presented here, a β-cell model (31), and a model for insulin kinetics (42). A detailed description of the homeostasis model is provided in APPENDIX C. The model was used to simulate two different conditions: an OGTT in a nondiabetic subject and a constant exogenous insulin infusion (310 pmol·min^{-1}·m^{-2}) in a T2D patient. The simulation was performed using both a saturable and a linear function for glucose uptake, and the two outcomes were compared.

RESULTS

Goodness of fit and model parameters. Table 2 shows the estimated typical values and inter-individual variability for the parameters of the model of glucose uptake (Eqs. 1 and 2), the half-lives of glucose and insulin concentrations at the site of action, and the glucose volume of distribution. Only one

Table 2. *Estimated typical values and interindividual variability for the main parameters of the glucose kinetics model*

Parameter	Typical Value[a]	Interquartile Range[b]
K_{mG} (mmol/l)	3.88	2.83–5.32
$V_{max,0}$ (mmol·min^{-1}·m^{-2})	0.338	NA[c]
E_{max} (mmol·min^{-1}·m^{-2})	4.81	3.84–6.03
K_{mI} (pmol/l)	784	555–1108
γ (dimensionless)	1.62	1.30–2.03
$t_{1/2,G}$ (min)[d]	0.7[e]	NA[c]
$t_{1/2,I}$ (min)[f]	15.9	12.3–20.7
V (liters)	12.7	10.8–14.8

[a]Estimated median of the probability distribution for the specific model parameter. [b]The range is computed based on the estimated variance of the probability distribution for the specific model parameter. [c]No interindividual variability was assumed for this parameter. [d]The corresponding half-life for the whole two-compartment delay model is 1.7 min. [e]This value was fixed. [f]The corresponding half-life for the whole two-compartment delay model is 38.5 (29.8–50.1) min.

correlation term on the probability distributions of the model parameters was found to be different from zero, namely, the correlation between K_{mI} and γ, estimated to be -0.44. The relative standard errors on the typical parameter estimates, evaluated by stochastic approximation, were less than 10% and those on the variability estimates were less than 30%.

The ability of the model to predict tracer concentrations in each test is shown in Fig. 3. On average, the model-predicted curves matched the experimental data closely with no systematic bias. Similarly, the model residuals, i.e., the difference between the measured and the predicted tracer concentration, were distributed around zero (not shown). Mean residuals were significantly different from zero only at very few time points, occurring mostly during the MTT/clamp study. When all the measurements and tests together were considered, the mean residual was less than 0.0001 mmol/l and its standard deviation was 0.014 mmol/l; the latter implies, relatively to the mean data, a coefficient of variation of 8%, which is of the same magnitude as the expected error on the tracer concentration measurement. This means that the model error could be mostly explained by the experimental error.

Glucose clearance. The time course of glucose clearance as predicted by the model (Fig. 1, *bottom* plot in each panel) illustrates how higher glucose concentrations can reduce the stimulating effect of hyperinsulinemia on glucose clearance; such effect was particularly evident during the first step of the HGclamp, where clearance failed to increase despite the rise in insulin, and at the beginning of the oral tests, where the increase in clearance was delayed compared with insulin concentration or clearance even decreased.

The suppression of glucose clearance due to uptake saturation with increasing glucose levels (Eq. 1) is depicted in Fig. 4: the steady-state relationship between glucose clearance and glucose concentration, as predicted by the model at an insulin concentration of 600 pmol/l, is shown for each subject in the different studies. When glucose concentration is raised from 5 to 10 mmol/l, glucose clearance is predicted to be reduced from 246 (185–348) ml·min^{-1}·m^{-2} to 158 (118–218) ml·min^{-1}·m^{-2} [median (interquartile range) from the individual curves]; the decrement averages 89 (66–130) ml·min^{-1}·m^{-2}.

The effect of insulin on the model parameter V_{max} (Eq. 2), representing maximal glucose uptake (Eq. 1), is depicted in Fig. 5: the individual model-derived curves show the variety of predicted sigmoidal effects and indicate that the HGclamp and ISOclamp are the two studies providing most of the data to identify the saturation of the insulin effect on glucose clearance, due to the higher insulin levels. In the other studies, V_{max} is extrapolated according to the population distribution of this parameter.

Role of BMI and study. The investigation of the effects of BMI and study on the model parameters showed that K_{mG} and K_{mI} were positively correlated with BMI ($P < 1e\text{-}7$ and $P = 0.0047$, respectively; adjusted $R^2 = 0.218$ and 0.148, respectively), and E_{max} was inversely correlated with BMI ($P = 0.0006$, adjusted $R^2 = 0.241$; see Table D1 in APPENDIX D). The study was a significant factor for K_{mG} ($P = 0.0011$) and E_{max}

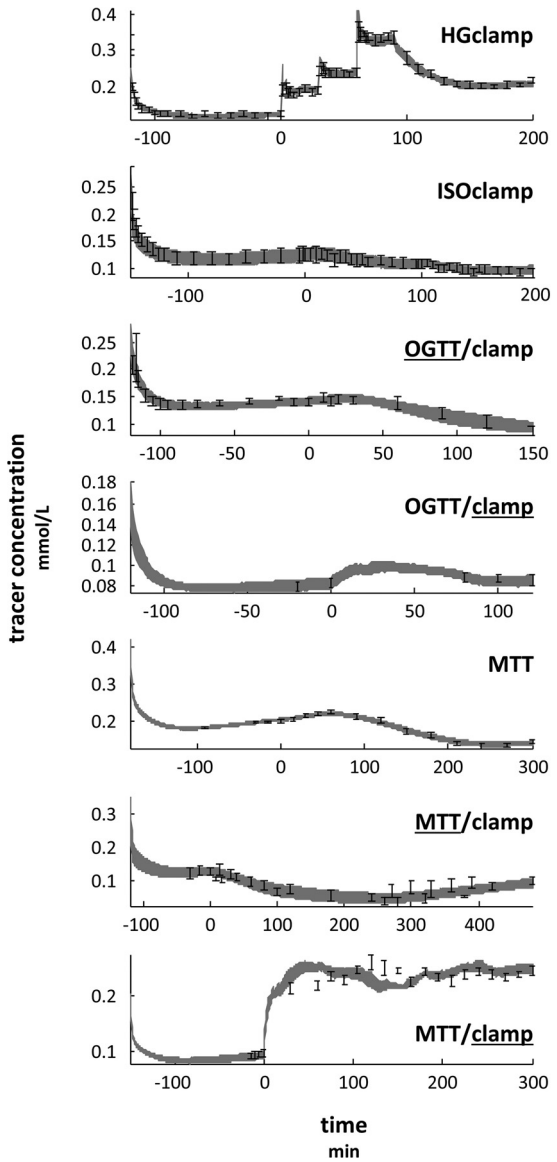

Fig. 3. Mean (±SE as error bars or gray areas) measured and model-predicted tracer concentrations during the 5 studies, as shown in the figure labels (see MATERIALS AND METHODS for abbreviations). Data were partially published previously (34, 16, 25); see APPENDIX A for details. The underlined text in the figure labels indicates the test in the 2 studies with paired tests (OGTT/clamp and MTT/clamp). T2D and ND subjects are not distinguished for clarity.

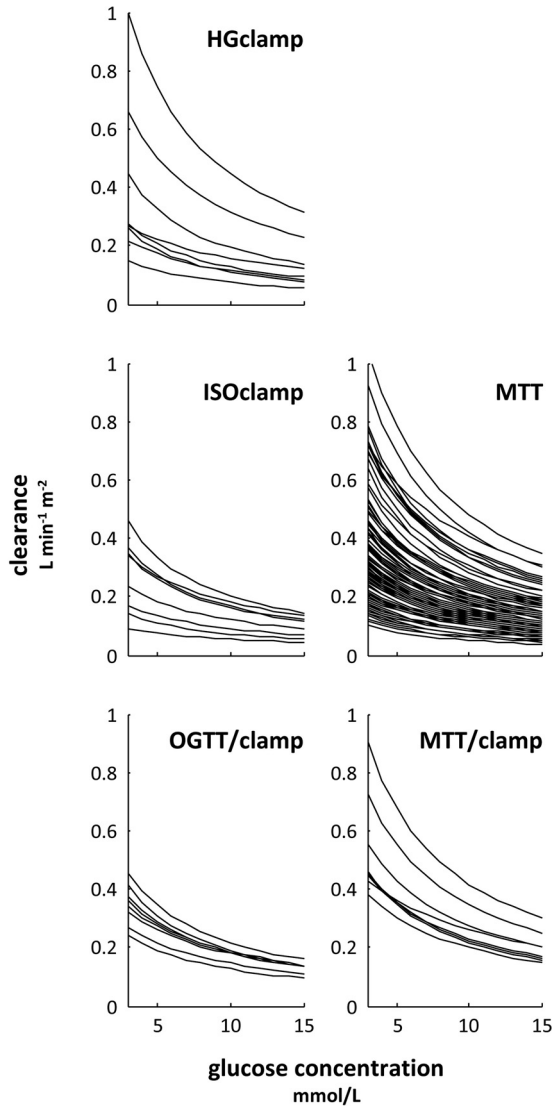

Fig. 4. Individual relationships between steady-state glucose clearance and glucose concentration as predicted by the model at a reference insulin concentration of 600 pmol/l in the 5 studies, as shown in the figure labels (see MATERIALS AND METHODS for abbreviations).

($P = 0.024$), although the BMI-adjusted differences between studies were modest (see Table D2 in APPENDIX D).

The model-derived estimates of a classical insulin sensitivity index from the euglycemic clamp, IS_{clamp}, and of standardized basal clearance, IS_b, were inversely correlated with BMI ($P = 0.0001$ and $P < 1e\text{-}7$, respectively; adjusted $R^2 = 0.234$ and 0.219, respectively; see Table D1 in APPENDIX D). The study did not affect IS_{clamp} or IS_b significantly.

Impact of uptake saturation on glucose levels. The simulation of an OGTT in a nondiabetic subject, using a saturable or a linear function for glucose uptake, predicted a maximum plasma glucose concentration of 9.38 vs. 8.63 mmol/l, respectively, and a mean plasma glucose concentration over the first 180 min of 7.73 vs. 7.06 mmol/l, respectively (Fig. 6*A*). A 310 pmol·min^{-1}·m^{-2} insulin infusion in a T2D patient with a fasting baseline plasma glucose of 10.0 mmol/l was predicted to result in a steady-state plasma glucose concentration of 6.33 mmol/l vs. 7.37 mmol/l, respectively (Fig. 6*B*).

DISCUSSION

The main result is that, despite a remarkable variety of experimental conditions, a unique mathematical model of glucose kinetics and insulin action was able to describe accurately and consistently the data from all subjects and tests. Moreover, the distributions of the individual parameter estimates were substantially homogeneous in the different studies; the differences in K_{mG} and E_{max}, although statistically significant, were small and did not undermine the consistency of the model.

Two specific features of the analysis are noteworthy. First, the model described both the intravenous and oral glucose tests with the same parameter distributions. Furthermore, when both oral and intravenous tests were performed in the same subject,

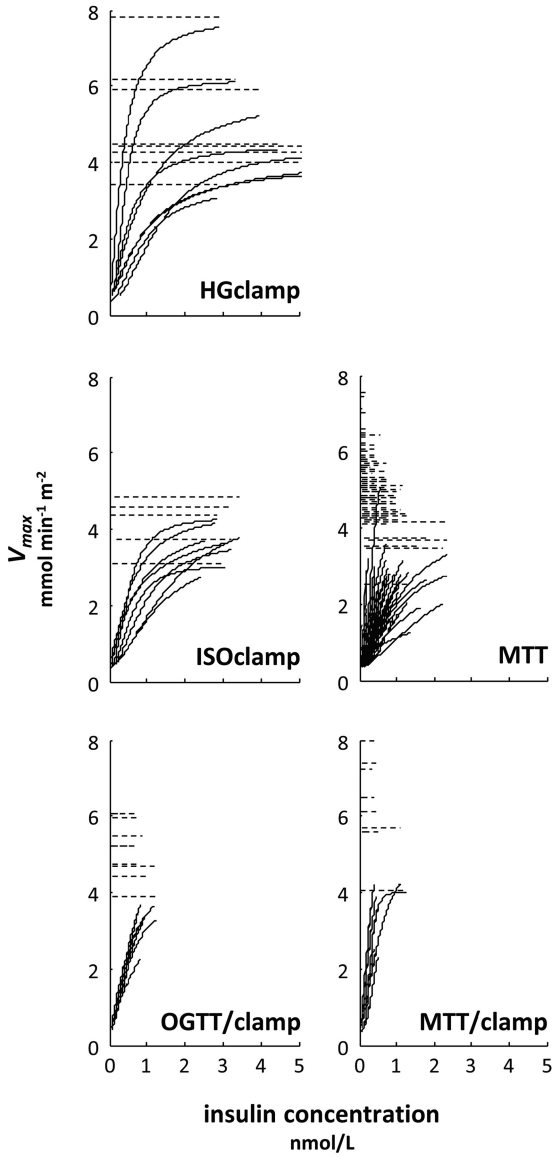

Fig. 5. Individual relationships between the parameter V_{max} and steady-state insulin concentration as computed by the model in the range of individually observed insulin values in the 5 studies, as shown in the figure labels (see MATERIALS AND METHODS for abbreviations). V_{max} represents the estimated maximal glucose uptake at glycemia levels approaching infinity. The dashed horizontal lines indicate the saturation values of the individual curves, and their length shows the observed insulin span.

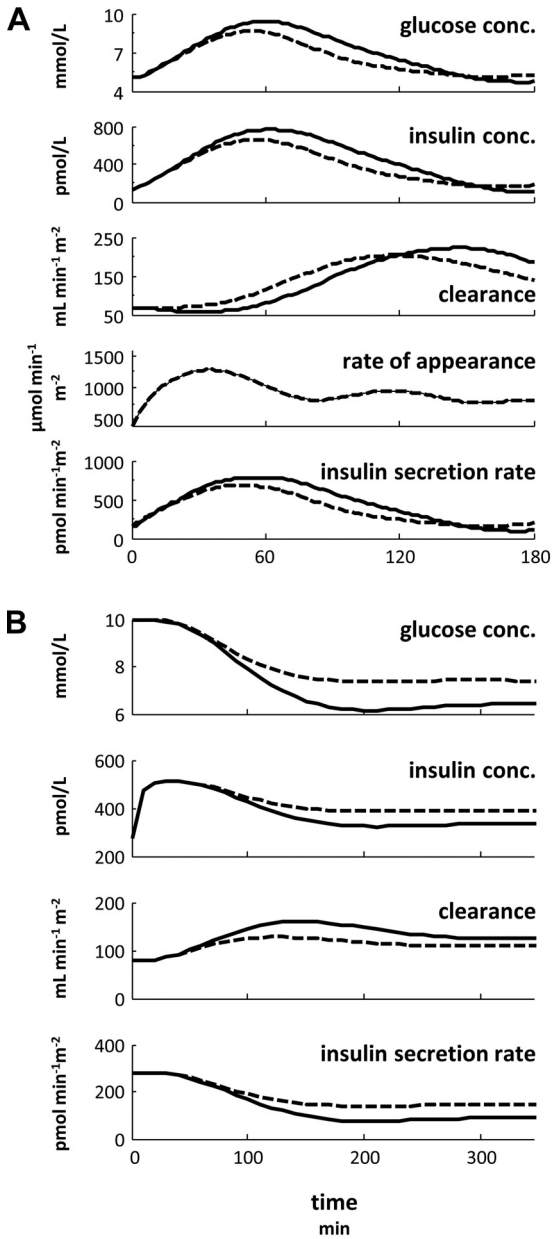

Fig. 6. Simulation of an oral glucose tolerance test in a ND subject (*A*) and of a constant insulin infusion in a T2D patient (*B*). Simulations with saturable (solid lines) and linear (dashed lines) glucose uptake are shown.

the same set of parameters described both data sets accurately. These results imply that the mechanisms underlying glucose uptake after oral and intravenous glucose administration can be described by the same model, a finding never reported before.

Second, the data set included tests (the hyperglycemic hyperinsulinemic clamp and the oral stimulations) in which, in the presence of hyperglycemia, hyperinsulinemia failed to increase glucose clearance as would be expected if glucose clearance were unaffected by the glucose levels. This phenomenon, confirmed by a previous independent analysis using a traditional tracer analysis approach (29), is well accounted for by the model of glucose utilization.

We observed a less accurate fit in the clamp data of the MTT/clamp study, as the predicted tracer concentration was oscillating around the measured values while the overall steady-state value was correctly captured. This oscillating deviation is unlikely to have originated from an inadequate model formulation. The lack of insulin sampling in the first 30 min may have limited the accuracy of the model prediction. It is also possible that transient variations during the clamp occurred for phenomena not related to the mechanisms we are describing (e.g., neurally mediated effects).

Our model, like all models in this area, necessarily involves simplifications. We used a circulatory model for glucose kinetics as a more physically oriented approach compared with compartmental models (27, 30). However, we did not attempt to describe the heterogeneity of organs lumped in the periphery block; therefore, the glucose utilization model does not make any explicit distinction between the various glucose-utilizing tissues (e.g., insulin-dependent and insulin-independent utilization). Nevertheless, our description is compatible with the coexistence of insulin-dependent and -independent utilization, as it assumes only that the two processes are saturable processes with similar Michaelis-Menten constants. Alternative assumptions could not be tested due to the lack of infrabasal insulin values, but our assumption can be justified by the similar affinities for glucose of GLUT4 and GLUT1, the main transporters involved in insulin-dependent and insulin-independent utilization, respectively (see below).

Despite the simplified description of glucose kinetics, the agreement with the previous studies is remarkable. The existence of saturation phenomena for glucose uptake in muscle cells was hypothesized a few decades ago (12) and clearly demonstrated in the whole body and in the forearm (44). The range of insulin and glucose concentrations levels covered in our studies is comparable with the conditions explored in previous studies; still, our analysis shows that a constant (i.e., not dependent on insulin) Michaelis-Menten parameter (K_{mG} in our mathematical model) is sufficient to describe the data. This concept, implying the same relative reduction in glucose clearance with hyperglycemia at all insulin levels, was anticipated by Fink et al. (19) and can be explained by the fact that under hyperinsulinemic conditions increased glucose entry into muscle is mainly due to the greater number of functioning GLUTs at the cell membrane (8). This corresponds to a constant K_{mG} and a V_{max} dependent on insulin concentration, as in our model. Other analyses have proposed different representations of this process (4, 12, 44). However, our model assumes for glucose utilization a saturable function of glucose and insulin concentrations at the site of action (i.e., delayed with respect to plasma concentrations), whereas the cited studies were based on the measured plasma concentrations. Moreover, the experimental procedures and the methods used to derive glucose uptake are different. Finally, the strength of our analysis is the use of individual estimates for K_{mG}, whereas previous studies computed a single K_m value for each insulin level by regressing mean or pooled glucose utilization against glucose levels.

Although the model does not have the ambition to strictly identify the Michaelis-Menten representation of glucose utilization with glucose transport, the interquartile range of the estimated individual values for K_{mG}, 2.83–5.32 mmol/l, is consistent with estimates of the affinity of the glucose transporters for glucose. Among this transporter family, GLUT4 is the main insulin-sensitive member, with highest expression in different tissues, including brown and white adipose tissue and

skeletal and cardiac muscle (45). GLUT1 is the most ubiquitously distributed GLUT isoform; it is involved in basal glucose uptake by most cells and cooperates with GLUT4 in insulin-sensitive tissues (45). The reported values for GLUT4's and GLUT1's K_m are rather variable, ranging between 2 and 5 mmol/l (8) and 5 and 6 mmol/l (23, 43) for GLUT4 and between 2 and 5 mmol/l (8) and 3 and7 mmol/l (45) for GLUT1. The similarity between our K_{mG} estimates and the K_m values reported for glucose transporters suggests that saturable glucose transport is the mechanism underlying the observed dependence of whole body glucose clearance on glucose concentration. In this respect, our study is more consistent with the in vitro data than the in vivo data by Yki-Järvinen et al. (44).

Maximal glucose uptake at a given insulin concentration, V_{max}, was assumed to depend on the insulin concentration at the site of action through a sigmoidal function with maximum value E_{max}. The shape of this function and the individual estimated values for its parameters correspond to those reported in previous studies on the effect of insulin on glucose uptake (2, 7, 19, 24, 37, 40). In particular, our glucose uptake model could accurately reproduce the individual data provided by Kolterman et al. (24) for both obese and nonobese subjects with glucose tolerance ranging from NGT to T2D (see Fig. D1 in APPENDIX D). Using the distributions estimated from our experiments as fixed prior probability distributions for the individual parameters values, all the individual estimates of E_{max}, K_{mI}, and γ obtained from Kolterman et al. data were in the range of those estimated from our data.

As further validation, we investigated the relationship between BMI and insulin sensitivity, as assessed by the model-predicted glucose clearance at 5 mmol/l glucose and 600 pmol/l insulin, a typical parameter of the hyperinsulinemic euglycemic glucose clamp. The expected negative correlation was reproduced, in accord with previous analyses on insulin sensitivity (17), and was homogeneous across all studies. Interestingly, the same relationship was also detected between BMI and the model-predicted glucose clearance at 5 mmol/l glucose and 71 pmol/l insulin, which is an estimate of insulin sensitivity under standardized basal conditions.

The effect of BMI on the model parameters was also investigated. BMI was found to be positively correlated with K_{mI}, the affinity of glucose uptake to insulin concentration, as expected (1, 6, 7, 14, 24, 34), and with K_{mG}, the affinity of glucose uptake to glucose concentration. Baron et al. (3) did not detect significant differences in the insulin K_m values of obese and lean subjects. However, comparison between the two studies is difficult because in our analysis most of the subjects (79%) had BMI above the obesity threshold used by Baron et al. (27 kg/m^2). Finally, in agreement with other work (1, 3, 6, 14, 24), we found an inverse correlation between BMI and E_{max}, the saturation level of glucose uptake produced by maximal insulin concentration.

The specific role of the glucose tolerance status was unclear in this study. In conditions standardized for glucose, insulin, and BMI, insulin sensitivity (IS_{clamp}) tended to be lower in diabetic patients than in normal subjects in the MTT/clamp study, but significance could not be achieved due to the small number of subjects. In the MTT study, a significant difference was not detected, possibly because of the mild diabetic status. While several studies have shown lower insulin sensitivity in diabetic patients (e.g., Ref. 3), this defect was not always detected, particularly in well-controlled, uncomplicated diabetes (35), as in our case. In contrast to a rather homogeneous distribution of BMI across the study groups, glucose tolerance was unbalanced, and this heterogeneity could have prevented the detection of differences. A similar unbalance concerned sex, for which we did not find the insulin sensitivity difference previously reported (21). On the other hand, the lack of dependence of insulin sensitivity on age (9, 10, 18, 33, 36) was observed also in this analysis.

Our study shows for the first time that saturation of glucose uptake may have a sizeable impact on glucose tolerance. In a simulation of a typical OGTT, compared with a model in which hyperglycemia does not suppress glucose clearance, our model predicts significantly higher glucose values ($\sim$0.7 mmol/l) despite compensatory insulin hypersecretion. An even greater impact was observed in the simulation of the effect of an exogenous insulin infusion in a diabetic patient: steady-state glycemia was 1.0 mmol/l lower than when no glucose uptake saturation was assumed. Although we do not provide an experimental proof of validity of these model predictions, the simulations emphasize the potential importance of the described phenomenon and suggest that it should be taken into account, for example when modeling glucose homeostasis or comparing conditions in which glucose levels differ.

The proposed model may have future applications in areas such as the development of more accurate insulin sensitivity indexes from tests other than the glucose clamp and for the study of insulin sensitivity in circumstances in which the glucose clamp would not be feasible or appropriate. Furthermore, the model may be an essential component of more accurate glucose homeostasis simulators, as exemplified by our prototype.

In summary, our analysis shows that glucose kinetics in euglycemic and hyperglycemic clamps and oral tests can be described by a single mechanism, consistent with the notions of glucose transport. Our mathematical model of glucose uptake reproduces specific and relevant features observed with concomitant hyperinsulinemia and hyperglycemia, in particular the glucose-induced reduction of glucose clearance. Finally, this model could allow better understanding of glucose metabolism and improved glucose homeostasis simulators.

APPENDIX A. EXPERIMENTAL PROTOCOLS AND ANALYTIC PROCEDURES

Three-Step Hyperglycemic Hyperinsulinemic Clamp (HGclamp)

The experimental procedures have been in part described previously (41). This analysis includes 8 of the 13 subjects participating in the original study (nondiabetic subjects with complete tracer data).

Experimental protocol. After an overnight fast, a primed (23.6 $\pm$ 2.4 μmol/kg) constant (0.22 $\pm$ 0.02 μmol$\cdot$min$^{-1}\cdot$kg^{-1}) infusion of [6,6-^{2}H$_2$]glucose was started and was continued for a 120-min basal period. Subsequently (from time $t = 0$), three consecutive 30-min square-wave steps of hyperglycemia were produced (on average 2.9, 5.8, and 10.6 mmol/l above baseline). Plasma glucose concentrations were maintained at the desired plateau by means of a variable 20% glucose infusion according to the glucose clamp technique (13). Each glucose infusion period was preceded by a priming dose to reach the target glucose level faster. The glucose infusate was enriched with [6,6-^{2}H$_2$]glucose to minimize changes in plasma [6,6-^{2}H$_2$]glucose enrichment. At $t = 90$, an intravenous bolus of 5 g of arginine followed, after 15–50 min, by a constant (24 pmol$\cdot$min$^{-1}\cdot$kg^{-1}) insulin infusion was given to raise glucose utilization to nearly maximal levels.

Two basal insulin samples and subsequent frequent blood samples were taken during the basal period for the determination of plasma glucose and [6,6-$^2H_2$]glucose concentration. Thereafter, blood samples were collected every 2 min for the first 10 min and every 5 min for another 20 min of each step of the clamp. After the arginine bolus, blood was sampled every 2 min for 10 min. During insulin infusion, blood was sampled every 10 min.

Analytic procedures. Plasma glucose was measured using the glucose oxidase method (Glucose Analyzer; Beckman Instruments, Fullerton, CA). Insulin was assayed in plasma by radioimmunoassay (Human Insulin-Specific RIA kit; Linco Research, St. Charles, MO). Enrichment of [6,6-$^2H_2$]glucose was measured by gas chromatography-mass spectrometry (GC-MS) (20). Briefly, after deproteinization, plasma samples were reacted with acetic anhydride and pyridine to form the pentaacetate derivative and measured by GC-MS (model 5972; Agilent, Fullerton, CA) using electron impact ionization and selective ion monitoring at mass-to-charge ratio 202/200.

Two-Step Isoglycemic Hyperinsulinemic Clamp (ISOclamp)

The experimental procedures have been described in detail previously (34).

Experimental protocol. Study participants were admitted to the unit in the morning after an overnight fast. The study protocol consisted of three periods: basal (from −145 to 0 min), low-insulin infusion (at a rate of 120 pmol·min^{-1}·m^{-2}, from 0 to 100 min), and high-insulin infusion (1,200 pmol·min^{-1}·m^{-2}, from 100 to 200 min). Each insulin infusion was primed with a bolus designed as fourfold the constant infusion rate for the first 4 min. At $t = -145$ min, a primed (25.6 ± 3.5 μmol/kg) constant (0.19 ± 0.06 μmol·min^{-1}·kg^{-1}) infusion of [6,6-$^2H_2$]glucose was started and was continued for the entire basal period. During insulin infusion, plasma glucose concentration was measured every 10 min and maintained at basal values by means of a variable 20% glucose infusion according to the isoglycemic clamp technique (13). To minimize the changes in plasma [6,6-$^2H_2$]glucose enrichment, 11 mmol of tracer was added to 500 ml of the 20% glucose solution, while the constant [6,6-$^2H_2$]glucose infusion was turned off in a stepwise fashion (by 25% every 10 min).

Blood sampling for the assay of plasma glucose, insulin, and [6,6-$^2H_2$]glucose enrichment was more frequent (every 2–5 min) during the first 50 min of each of the three study periods and was spaced at 10- to 15-min intervals thereafter. During the basal period, four to five blood samples were taken for plasma insulin determination, and more frequent samples were taken for the assay of plasma glucose and [6,6-$^2H_2$]glucose enrichment.

Analytic procedures. Plasma glucose was measured using the glucose oxidase method (Glucose Analyzer, Beckman Instruments, Fullerton, CA). Insulin was assayed in plasma by RIA (Human Insulin-specific RIA kit from Linco Research). Plasma [6,6-$^2H_2$]glucose enrichment was measured in arterialized blood samples after deproteinization with barium hydroxide (0.3 N) and zinc sulfate (0.3 N). Enrichment of [6,6-$^2H_2$]glucose was measured by GC-MS (20). Briefly, after deproteinization, plasma samples were reacted with acetic anhydride and pyridine to form the pentaacetate derivative and measured by GC-MS (model 5972, Agilent) using electron-impact ionization and selective ion monitoring at mass-to-charge ratio 202/200.

Paired Oral Glucose Tolerance Test and Euglycemic Hyperinsulinemic Clamp (OGTT/clamp)

This study was part of an ancillary protocol of the RISC study (22), and its experimental procedures have been described in detail previously (15).

Experimental protocol. CLAMP. In the morning after an overnight fast, a primed [22.2 ± 0.5 μmol per kilogram of estimated lean body mass (LBM)] constant (0.19 ± 0.05 μmol·min^{-1}·kg$_{LBM}^{-1}$) infusion of [6,6-$^2H_2$]glucose was started. After a 2-h equilibration period, a primed, continuous infusion of insulin at a rate of 240 pmol·min^{-1}·m^{-2} was given simultaneously with a variable 20% dextrose infusion adjusted every 5 min to maintain plasma glucose levels within 0.8 mmol/l (±15%) of the target glucose level (4.5–5.5 mmol/l). The glucose infusate was enriched with [6,6-$^2H_2$]glucose to minimize changes in plasma [6,6-$^2H_2$]glucose enrichment. Plasma samples for the measurement of glucose, [6,6-$^2H_2$]glucose, and insulin were taken during the basal period (−20 to 0 min) and at the end of the clamp (80 to 120 min). Glucose was additionally measured every ~5 min during the clamp.

OGTT. In the morning after an overnight fast, a primed (36.8 ± 9.6 μmol/kg$_{LBM}$) constant (0.34 ± 0.04 μmol·min^{-1}·kg$_{LBM}^{-1}$) infusion of [6,6-$^2H_2$]glucose was started. After a 2-h equilibration period, a 75-g OGTT was given. Plasma samples for the measurement of glucose and [6,6-$^2H_2$]glucose were taken frequently during the 2-h equilibration period. Three basal insulin samples were also taken. During the OGTT period (0–150 min), plasma samples were taken at 5- to 30-min intervals for measurement of glucose, insulin, and the glucose tracer.

Analytic procedures. Plasma glucose was measured using the glucose oxidase technique (Glucose Analyzer;Beckman Instruments, Fullerton, CA). OGTT plasma insulin was measured in duplicate by RIA using a kit for human insulin with negligible cross-reactivity with proinsulin and its split products (Linco Research, St. Charles, MO). Clamp plasma insulin was measured in the central laboratory of the RISC study by a two-sited, time-resolved fluoroimmunoassay (AutoDELFIA Insulin kit; Wallac Oy, Turku, Finland) using monoclonal antibodies. As this insulin assay provided values lower than the assay used in the OGTT, a calibration curve against the Linco RIA kit was constructed, and the DELFIA values were converted to the Linco scale. The calibration curve was based on paired measurements of the same pool of 50 plasma samples spanning a wide insulin concentration range (50-1,000 pmol/l). The two measurements were strongly linearly related ($R = 0.99$).

Enrichment of [6,6-$^2H_2$]glucose was measured by GC-MS (20). Briefly, after deproteinization, plasma samples were reacted with acetic anhydride and pyridine to form the pentaacetate derivative and measured by GC-MS (model 5972, Agilent) using electron impact ionization and selective ion monitoring at mass-to-charge ratio 202/200.

Mixed-Meal Test (MTT)

The experimental procedures have been described in detail previously (16). This analysis includes the baseline data of all diabetic patients of the original study plus 25 nondiabetic subjects studied with the same protocol.

Experimental protocol. The study consisted of a 5-h meal tolerance test following a 3-h basal period combined with a glucose tracer. A primed (~28 μmol/kg × FPG/5, where FPG is fasting plasma glucose in mmol/l) constant (~0.28 μmol·min^{-1}·kg^{-1}) infusion of [6,6-$^2H_2$]glucose was administered starting at $t = -180$ min during the whole test. At *time 0*, subjects ingested (in <10 min) a meal consisting of 1 egg, 50 g parmesan cheese, 50 g white bread, and 75 g glucose in water (total calorie content 710 kcal: 58% carbohydrate, 24% fat, 18% protein). Four blood samples were taken before the beginning of the meal to measure plasma glucose, tracer, and insulin concentrations in the fasting state. Afterward, blood samples were collected every 15 min during the first hour and every 30 min until the end of the test.

Analytic procedures. Tracer enrichment of [6,6-$^2H_2$]glucose was measured by GC-MS (Finnigan Trace GC/DSQ, Thermo Electron) using electron impact ionization and selective ion monitoring at mass-to-charge ratios 202/200 (20). Plasma glucose concentrations were measured by a chemical enzymatic method on a Synchron

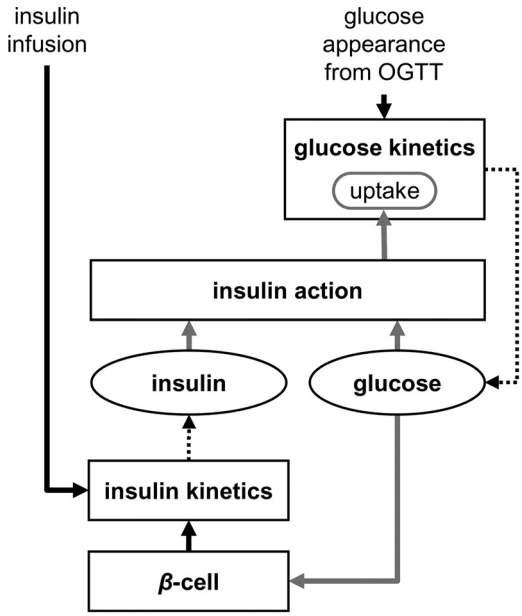

Fig. C1. Prototypical glucose homeostasis model used to simulate glucose and insulin concentrations with or without saturation of glucose uptake. In the OGTT simulation, the glucose rate of appearance is the input of the glucose kinetics submodel, implemented as described in this article. The output of this submodel, plasma glucose concentration, drives the β-cell submodel and affects insulin action on glucose uptake. The β-cell submodel predicts insulin secretion, which is the input of the submodel describing insulin kinetics. The insulin kinetics submodel provides plasma insulin concentration, which is the second input required by the insulin action module. In the simulation of exogenous insulin infusion, the glucose rate of appearance (glucose production) is constant, and the rate of insulin infusion is a further input of the insulin kinetics module.

Clinical System CX4 (Beckman Instruments). Plasma insulin was assayed by chemiluminescence (COBAS e411 Instrument, Roche).

Paired MMT and Hyperglycemic Hyperinsulinemic Clamp (MTT/clamp)

The experimental procedures have been described in detail previously (25). This analysis includes all subjects for whom both a MMT and hyperglycemic hyperinsulinemic clamp were available.

Experimental protocol. MMT. Each subject was served breakfast (231 kcal, 7:00 AM) and lunch (208 kcal, 11:00 AM). At 3:00 PM, a primed (~20 μmol/kg in normoglycemic subjects and 20 μmol/kg × FPG/5 in diabetic subjects, where FPG is fasting plasma glucose in mmol/l) constant (~0.20 μmol kg^{-1} min^{-1}) infusion of [6,6-$^2H_2$]glucose was started. At 5:00 PM ($t = 0$), the test meal (400 ml liquid meal, 652 kcal; carbohydrate:protein:fat: 83.6 g/23.2 g/24.0 g) was ingested. After dinner, the [6,6-$^2H_2$]glucose infusion rate was stepwise adjusted according to a protocol developed in pilot experiments ($n = 5$) aimed at minimizing variations of the tracer-to-tracee ratio of endogenous glucose.

Plasma glucose, tracer, and insulin concentrations in the fasting state were measured five, three, and one times, respectively. Afterward, glucose and tracer concentration were measured approximately 10 times in the first 2 h and 10 times in the last 6 h; insulin concentration was measured at $t = 30$ and 60 min and then every hour.

CLAMP. Subsequently, T2D patients were admitted the evening before the clamp study, and plasma glucose concentrations were normalized overnight using intravenous insulin infusion. Nondiabetic volunteers were admitted at 6:00 AM the day of the study. At 6:30 AM ($t = -150$ min), a primed (~20 μmol/kg) constant (~0.20 μmol·kg^{-1}·min^{-1}) infusion of [6,6-$^2H_2$]glucose was started. At 9:00 AM (0 min), a hyperglycemic hyperinsulinemic pancreatic clamp test was initiated by somatostatin infusion (at a rate of 0.1 μg·kg^{-1}·min^{-1}, from −5 to 300 min); and insulin infusion (at a rate of 480 pmol/min per m^2 of body surface area (BSA) from 0 to 8 min; at a rate of 240 pmol/min per m^2 of BSA from 8 to 300 min). Plasma glucose was raised and maintained at ~10 mmol/l (~180 mg/dl) by primed variable 20% dextrose infusion enriched with [6,6-$^2H_2$]glucose.

Plasma samples for the measurement of [6,6-$^2H_2$]glucose were taken four times every 5 min before the start of the clamp, at $t = 30$ and 60 min, and every 15 min afterward. Glucose was additionally measured every 5 min during the clamp. Insulin samples were taken at $t = -180$, −15, 0, 30, and 60 min, and every hour afterward.

Analytic procedures. Plasma glucose was measured using the glucose oxidase method (Glucose Analyzer II, Beckman Instruments, Fullerton, CA). Plasma immunoreactive insulin was measured by commercially available RIAs (38, 39). Enrichment of [6,6-$^2H_2$]glucose was measured by GC-MS (5). Briefly, after deproteinization, plasma samples were derivatized as glucose pentaacetate and analyzed on a Hewlett-Packard 5890 gas chromatograph using electron impact ionization and selective ion monitoring at mass-to-charge ratio 187/189.

APPENDIX B. THE CIRCULATORY MODEL OF GLUCOSE KINETICS

The circulatory model includes two interconnected blocks: a heart-lung (HL) block and a periphery (PER) block, which lumps together all the remaining tissues. Each block is regarded as a single inlet-single outlet organ and can be described mathematically by an impulse response (27). The organ impulse response is defined as the tracer efflux observed at the outlet after a bolus injection of a unit dose into the inlet (with assumption of no tracer recirculation). After bolus injection into a peripheral vein, the tracer disappearance curve is the result of the combination of the impulse responses of the two interconnected blocks. Cardiac output (F) was assumed to remain constant during each test and was assumed to be 3,200 ml/min per m^2 of BSA (34) multiplied by the ratio of whole blood to plasma glucose concentration (BP = 0.84) to obtain the actual glucose mass flux from the measurement of tracer in plasma.

The impulse response of the HL block was assumed to be known and not affected by insulin or glucose. It was represented by a two-exponential function starting from zero and returning to zero after rising to an early peak. The parameters of the HL impulse response were set to match experimentally derived curves, as detailed in McGuinness and Mari (32). In particular, HL glucose distribution volume (V_{HL}) was assumed to be 700 ml/m^2, glucose fractional extraction was assumed to be zero, and the exponent δ_{HL} of the rising exponential term was fixed to 15 min^{-1}. The impulse response of the periphery block was represented by a four-exponential function,

Table D1. *Influence of BMI on the model parameters*, IS_{clamp}, and IS_b, from N-way ANOVA*

	BMI 27.7 kg/m²†	BMI 35.0 kg/m²‡
K_{mG} (pmol/l)	3.69	4.22
E_{max} (mmol·min^{-1}·m^{-2})	4.80	4.35
K_{mI} (pmol/l)	690	816
IS_{clamp} (ml·min^{-1}·m^{-2})	261	199
IS_b (ml·min^{-1}·m^{-2})	56	45

IS_{clamp}, model-derived glucose clearance at 5 mmol/l glucose and 600 pmol/l insulin; IS_b, model-derived glucose clearance at 5 mmol/l glucose and 71 pmol/l insulin. *Parameters for which a significant BMI effect was detected. †BMI value corresponding to the 25th %-ile in the studied population. ‡BMI value corresponding to the 75th %-ile in the studied population.

Table D2. *BMI-adjusted values* for K_{mG} and E_{max} in the different studies† for normal glucose regulation subjects*

	HGclamp	ISOclamp	OGTT/Clamp	MTT	MTT/clamp
K_{mG} (mmol/l)	2.93 (2.18–3.93)	3.75 (2.74–5.12)	4.49 (3.38–5.97)	3.46 (2.84–4.21)	3.92 (2.88–5.35)
E_{max} (mmol·min^{-1}·m^{-2})	4.77 (3.64–6.25)	3.86 (2.89–5.17)	4.54 (3.45–5.99)	4.66 (3.86–5.62)	5.36 (4.02–7.14)

Values are given as mean (95% confidence interval), as computed from *N*-way ANOVA, on the individual parameter estimates, for a BMI reference value of 29.7 kg/m^2. †See MATERIALS AND METHODS for abbreviations.

starting from zero and gradually returning to zero after reaching a peak, with the fastest rising exponential term fixed. This impulse response can be conveniently represented as a convolution of a three-exponential function and a single-exponential function, $\delta e^{-\delta t}$, representing the fastest rising exponential term in which $\delta = 10$ min^{-1} is fixed (32). Thus,

$$r_{PER}(t) = \delta e^{-\delta t} \otimes \left[w_1\lambda_1 e^{-\lambda_1 t} + w_2\lambda_2 e^{-\lambda_2 t} + w_3\lambda_3 e^{-\lambda_3 t}\right]\left(1 - E\right),$$

where the symbol $\otimes$ is the convolution operator. In the three-exponential function in square brackets, it is assumed that the sum of the parameters w_i is 1. With this assumption, its integral from zero to infinity is 1, and w_i represent the relative contribution of the exponential terms of exponents λ_i to the total integral. It follows that the integral from zero to infinity of $r_{PER}(t)$ is 1-$E(t)$; i.e., $E(t)$ is the glucose fractional extraction of the periphery block (32).

The state space representation of the whole system is the following:

$$\dot{x}_{HL}(t) = A_{HL}x_{HL}(t) + B_{HL}\left(G^*_v(t) + \varphi_i(t)/F\right)$$

$$G^*(t) = C_{HL}x_{HL}(t)$$

$$\dot{x}_{PER}(t) = A_{PER}x_{PER}(t) + B_{PER}\left(1 - E(t)\right)G^*(t)$$

$$G^*_v(t) = C_{PER}x_{PER}(t)$$

where

$$x_{HL}(0) = \begin{bmatrix} \varphi_b/F \\ \varphi_b/F \end{bmatrix},$$

$$x_{PER}(0) = \begin{bmatrix} 0 \\ 0 \\ 0 \\ 0 \end{bmatrix},$$

$$E(t) = cl(t)/F,$$

$$A_{HL} = \begin{bmatrix} c2 & 0 \\ 0 & -\delta_{HL} \end{bmatrix},$$

$$B_{HL} = \begin{bmatrix} 1 \\ 1 \end{bmatrix},$$

$$C_{HL} = \begin{bmatrix} c1 & -c1 \end{bmatrix},$$

$$c1 = \frac{\delta_{HL} \times F}{\delta_{HL} \times V_{HL} - 2 \times F},$$

$$c2 = -\frac{\delta_{HL} \times F}{\delta_{HL} \times V_{HL} \times F},$$

$$A_{PER} = \begin{bmatrix} -\lambda_1 & 0 & 0 & 0 \\ 0 & -\lambda_2 & 0 & 0 \\ 0 & 0 & -\lambda_3 & 0 \\ \lambda_1 & \lambda_2 & \lambda_3 & -\delta \end{bmatrix},$$

$$B_{PER} = \begin{bmatrix} w_1 \\ w_2 \\ w_3 \\ 0 \end{bmatrix},$$

$$C_{PER} = \begin{bmatrix} 0 & 0 & 0 & \delta \end{bmatrix}.$$

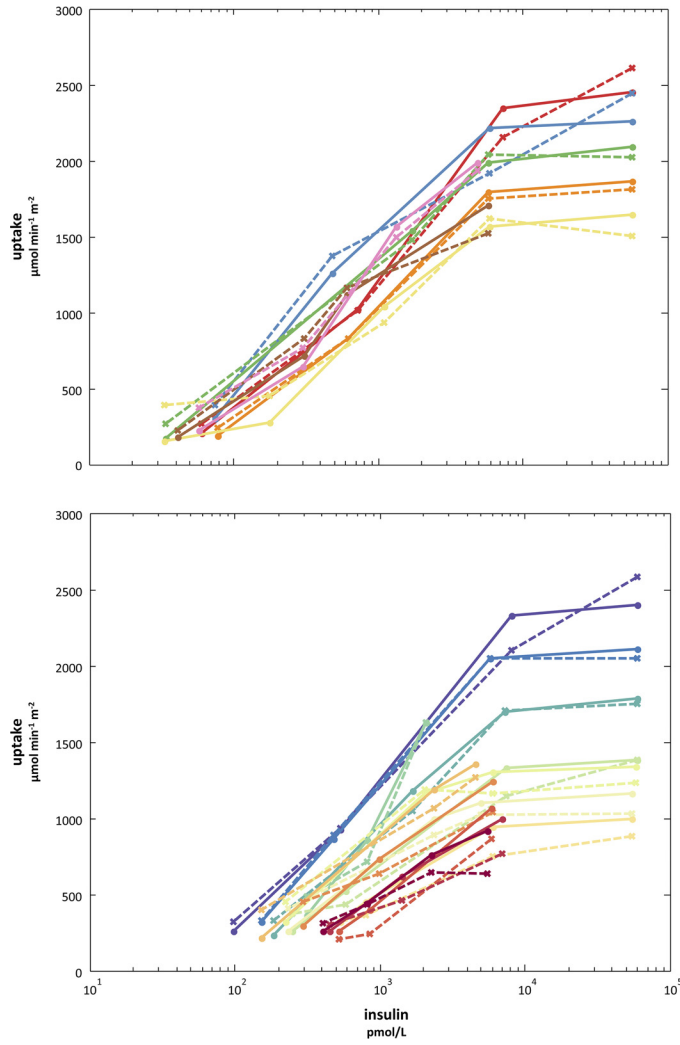

Fig. D1. Crosses connected by dashed lines: glucose uptake measured by Kolterman at al. (24) in nonobese (*top*) and obese (*bottom*) subjects undergoing euglycemic clamps at different insulin infusion rates. Dots connected by solid lines: model prediction of glucose uptake for the reported insulin and glucose levels. The individual parameter estimates were obtained by fitting the model to the data according to a maximum a posteriori approach and using the parameter distributions identified from our studies as priors.

In the previous equations, *cl(t)* is the glucose clearance computed by the glucose clearance model described in MATERIALS AND METHODS (Eq. 3); G^* and G_v^* are the arterial and mixed venous glucose tracer concentrations, respectively (mmol/l), $\varphi_i(t)$ is the tracer infusion ($\mu mol \cdot min^{-1} \cdot m^{-2}$), and φ_b is the tracer bolus ($\mu mol/m^2$) applied at the beginning of the test.

From the expression for the glucose volume of distribution V:

$$V = V_{HL} + F \times \left(\frac{1}{\delta} + \sum_i \frac{w_i}{\lambda_i} \right),$$

the following reparameterization of w_2, w_3, λ_1, λ_2, and λ_3 were obtained:

$$w_2 = (1 - w_1) \times f_{w_2},$$

$$w_3 = 1 - w_1 - w_2,$$

$$\lambda_1 = \frac{(w_1 \times f_{\lambda_2} \times f_{\lambda_3} + w_2 \times f_{\lambda_3} + w_3)}{f_{\lambda_2} \times f_{\lambda_3}} \times \frac{\delta \times F}{\delta \times (V - V_{HL}) - F},$$

$$\lambda_2 = \lambda_1 \times f_{\lambda_2},$$

$$\lambda_3 = \lambda_2 \times f_{\lambda_3}.$$

These equations, together with the logit distributions of w_1, f_{w2}, $f_{\lambda 2}$, and $f_{\lambda 3}$ constraining their values to be between 0 and 1, ensure that $\lambda_1 > \lambda_2 > \lambda_3$, which is required to avoid identifiability issues, and that the sum of the w_i is 1.

The parameters to be estimated in the whole circulatory model for glucose kinetics were thus V, w_1, f_{w2}, $f_{\lambda 2}$, and $f_{\lambda 3}$.

The transit compartment models for glucose and insulin at the site of action were represented with the following equations:

$$\frac{dX_1}{dt} = \frac{ln(2)}{t_{1/2,G}} [G(t) - X_1(t)], X_1(0) = G(0),$$

$$\frac{dX}{dt} = \frac{ln(2)}{t_{1/2,G}} [X_1(t) - X(t)], X(0) = G(0),$$

$$\frac{dZ_1}{dt} = \frac{ln(2)}{t_{1/2,i}} [I(t) - Z_1(t)], Z_1(0) = I(0),$$

$$\frac{dZ}{dt} = \frac{ln(2)}{t_{1/2,i}} [Z_1(t) - Z(t)], Z(0) = I(0),$$

where *G(t)* is the plasma glucose concentration, *I(t)* is the plasma insulin concentration, and $t_{1/2,G}$ and $t_{1/2,I}$ are the compartment half-times for glucose and insulin action, respectively. The initial conditions in the four equations above represent the steady state at *time 0*.

APPENDIX C. ASSESSMENT OF THE EFFECTS OF GLUCOSE UPTAKE SATURATION ON GLUCOSE LEVELS

A simplified prototype of a glucose homeostasis model was developed assembling the complete glucose kinetics model of this study, a model of insulin kinetics (42), and a model of insulin secretion (31) (Fig. C1). In the original model of insulin secretion (31), potentiation is a time-dependent function that cannot be predicted from glucose. In the simulations described below, we thus used a simplified representation with no potentiation effects (i.e., potentiation equal to one).

To evaluate the effects of glucose uptake saturation, two simulations were performed, one with the original glucose uptake model (Eq. 1, and the connected Eq. 3 for glucose clearance) and one in which glucose uptake was linearized; i.e., glucose clearance was made glucose independent by fixing the glucose term at the denominator of the Michaelis-Menten equation to the basal value:

$$\varphi(t) = \frac{V_{max}(t) X(t)}{K_{mG} + G(0)},$$

$$cl(t) = \frac{V_{max}(t)}{K_{mG} + G(0)},$$

In these simulations, the model was used to predict glucose concentration in place of tracer concentration, assuming a known rate of glucose appearance (see below). The initial conditions for the model variables x_{HL} and x_{PER} (see APPENDIX B) were set to empirical values and the simulation started much earlier than *time 0*, to ensure a steady-state condition at *time 0*.

Two experimental conditions were simulated: an OGTT in a nondiabetic subject and an exogenous insulin infusion in a diabetic subject in fasting conditions. The parameter values for the glucose kinetics model were set to the estimated typical values (Table 2). The insulin kinetics parameters were taken from Tura et al. (42). The β-cell model parameters were chosen as the mean values reported by Mari et al. (31) for control and T2D subjects, in the simulation of the OGTT and the insulin infusion, respectively: β-cell glucose sensitivity = 148 and 53 $pmol \cdot m^{-2}\ mM^{-1}$, respectively; rate sensitivity = 908 and 220 $pmol \cdot m^{-2}\ mM^{-1}$, respectively; secretion at 5 mmol/l glucose for the OGTT simulation = 136 $pmol \cdot min^{-1} \cdot m^{-2}$; secretion at 10 mmol/l glucose for the insulin infusion simulation = 279 $pmol \cdot min^{-1} \cdot m^{-2}$. Glucose concentration was fixed to 5 mmol/l before the OGTT and to 10 mmol/l before the insulin infusion. In the OGTT simulation, the glucose rate of appearance was computed before the test as the value producing the imposed basal glucose concentration, and afterward as the mean in the volunteers from the OGTT/clamp study (Fig. 6*A*). In the glucose infusion simulation, the glucose production was set to the constant value producing the imposed basal glucose concentration.

APPENDIX D. SUPPLEMENTARY ANALYSES

Tables D1 and D2 extend the findings presented in RESULTS, providing insight on the role of BMI and study on the model parameters, on the insulin sensitivity index from the euglycemic clamp, IS_{clamp}, and on the standardized basal clearance, IS_b.

Figure D1 shows the fit of the individual glucose uptake curves from the study by Kolterman et al. (24) for obese and nonobese subjects with glucose tolerance ranging from NGT to T2D, obtained with our model as described in the DISCUSSION.

ACKNOWLEDGMENTS

We acknowledge Toni Giorgino PhD for technical support in using the software adopted for the analysis. We acknowledge the CINECA award under the ISCRA initiative, for the availability of high performance computing resources and support.

GRANTS

This research received support from the Innovative Medicines Initiative Joint Undertaking under Grant Agreement no. 115156, resources of which are composed of financial contribution from the European Union's Seventh Framework Programme (FP7/2007–2013) and EFPIA companies' in-kind contribution. The DDMoRe project is also financially supported by contributions from Academic and SME partners.

DISCLOSURES

No conflicts of interest, financial or otherwise, are declared by the author(s).

AUTHOR CONTRIBUTIONS

R.B. and A.M. conception and design of research; R.B. and A.M. analyzed data; R.B., A.N., E.F., and A.M. interpreted results of experiments; R.B. prepared figures; R.B. and A.M. drafted manuscript; R.B., A.N., E.O.A.M., M.R., E.F., and A.M. edited and revised manuscript; R.B., A.N., A.G., E.O.A.M., M.K., A.B., M.R., E.F., and A.M. approved final version of manuscript; A.N., A.G., E.O.A.M., M.K., A.B., and M.R. performed experiments.

REFERENCES

1. **Baron AD.** Hemodynamic actions of insulin. *Am J Physiol Endocrinol Metab* 267: E187–E202, 1994.
2. **Baron AD, Kolterman OG, Bell J, Mandarino LJ, Olefsky JM.** Rates of noninsulin-mediated glucose uptake are elevated in type II diabetic subjects. *J Clin Invest* 76: 1782–1788, 1985.
3. **Baron AD, Laakso M, Brechtel G, Edelman SV.** Reduced capacity and affinity of skeletal muscle for insulin-mediated glucose uptake in noninsulin-dependent diabetic subjects. Effects of insulin therapy. *J Clin Invest* 87: 1186–1194, 1991.
4. **Best JD, Taborsky GJ Jr, Halter JB, Porte D Jr.** Glucose disposal is not proportional to plasma glucose level in man. *Diabetes* 30: 847–850, 1981.
5. **Bischof MG, Bernroider E, Krssak M, Krebs M, Stingl H, Nowotny P, Yu C, Shulman GI, Waldhäusl W, Roden M.** Hepatic glycogen metabolism in type 1 diabetes after long-term near normoglycemia. *Diabetes* 51: 49–54, 2002.
6. **Bogardus C, Lillioja S, Mott D, Reaven GR, Kashiwagi A, Foley JE.** Relationship between obesity and maximal insulin-stimulated glucose uptake in vivo and in vitro in Pima Indians. *J Clin Invest* 73: 800–805, 1984.
7. **Bonadonna RC, Leif G, Kraemer N, Ferrannini E, Prato SD, DeFronzo RA.** Obesity and insulin resistance in humans: a dose-response study. *Metabolism* 39: 452–459, 1990.
8. **Bouché C, Serdy S, Kahn CR, Goldfine AB.** The cellular fate of glucose and its relevance in type 2 diabetes. *Endocr Rev* 25: 807–830, 2004.
9. **Broughton DL, Taylor R.** Review: deterioration of glucose tolerance with age: the role of insulin resistance. *Age Ageing* 20: 221–225, 1991.
10. **Coon PJ, Rogus EM, Drinkwater D, Muller DC, Goldberg AP.** Role of body fat distribution in the decline in insulin sensitivity and glucose tolerance with age. *J Clin Endocrinol Metab* 75: 1125–1132, 1992.
11. **Dalla Man C, Rizza RA, Cobelli C.** Meal simulation model of the glucose-insulin system. *IEEE Trans Biomed Eng* 54: 1740–1749, 2007.
12. **DeFronzo RA, Ferrannini E.** Influence of plasma glucose and insulin concentration on plasma glucose clearance in man. *Diabetes* 31: 683–688, 1982.
13. **DeFronzo RA, Tobin JD, Andres R.** Glucose clamp technique: a method for quantifying insulin secretion and resistance. *Am J Physiol Endocrinol Metab Gastrointest Physiol* 237: E214–E223, 1979.
14. **Devlin JT, Horton ES.** Effects of prior high-intensity exercise on glucose metabolism in normal and insulin-resistant men. *Diabetes* 34: 973–979, 1985.
15. **Ferrannini E, Balkau B, Coppack SW, Dekker JM, Mari A, Nolan J, Walker M, Natali A, Beck-Nielsen H, Investigators RISC .** Insulin resistance, insulin response, and obesity as indicators of metabolic risk. *J Clin Endocrinol Metab* 92: 2885–2892, 2007.
16. **Ferrannini E, Muscelli E, Frascerra S, Baldi S, Mari A, Heise T, Broedl UC, Woerle HJ.** Metabolic response to sodium-glucose cotransporter 2 inhibition in type 2 diabetic patients. *J Clin Invest* 124: 499–508, 2014.
17. **Ferrannini E, Natali A, Bell P, Cavallo-Perin P, Lalic N, Mingrone G.** Insulin resistance and hypersecretion in obesity. European Group for the Study of Insulin Resistance (EGIR). J *Clin Invest* 100: 1166–1173, 1997.
18. **Ferrannini E, Vichi S, Beck-Nielsen H, Laakso M, Paolisso G, Smith U.** Insulin action and age. European Group for the Study of Insulin Resistance (EGIR). *Diabetes* 45: 947–953, 1996.
19. **Fink RI, Wallace P, Brechtel G, Olefsky JM.** Evidence that glucose transport is rate-limiting for in vivo glucose uptake. *Metabolism* 41: 897–902, 1992.
20. **Gastaldelli A, Casolaro A, Pettiti M, Nannipieri M, Ciociaro D, Frascerra S, Buzzigoli E, Baldi S, Mari A, Ferrannini E.** Effect of pioglitazone on the metabolic and hormonal response to a mixed meal in type II diabetes. *Clin Pharmacol Ther* 81: 205–212, 2007.
21. **Geer EB, Shen W.** Gender differences in insulin resistance, body composition, and energy balance. *Gend Med* 6, *Suppl* 1: 60–75, 2009.
22. **Hills SA, Balkau B, Coppack SW, Dekker JM, Mari A, Natali A, Walker M, Ferrannini E, Study Group EGIRRISC.** The EGIR-RISC STUDY (The European Group for the Study of Insulin Resistance: relationship between insulin sensitivity and cardiovascular disease risk). I. Methodology and objectives. *Diabetologia* 47: 566–570, 2004.
23. **Kasahara T, Kasahara M.** Characterization of rat Glut4 glucose transporter expressed in the yeast *Saccharomyces cerevisiae*: comparison with Glut1 glucose transporter1. *Biochim Biophys Acta BBA-Biomembr* 1324: 111–119, 1997.
24. **Kolterman OG, Insel J, Saekow M, Olefsky JM.** Mechanisms of insulin resistance in human obesity: evidence for receptor and postreceptor defects. *J Clin Invest* 65: 1272–1284, 1980.
25. **Krssak M, Brehm A, Bernroider E, Anderwald C, Nowotny P, Dalla Man C, Cobelli C, Cline GW, Shulman GI, Waldhäusl W, Roden M.** Alterations in postprandial hepatic glycogen metabolism in type 2 diabetes. *Diabetes* 53: 3048–3056, 2004.
26. **Lixoft.** MONOLIX. [Online] http://wwwlixoft.eu/products/monolix/product-monolix-overview/.
27. **Mari A.** Circulatory models of intact-body kinetics and their relationship with compartmental and non-compartmental analysis. *J Theor Biol* 160: 509–531, 1993.
28. **Mari A.** Determination of the single-pass impulse response of the body tissues with circulatory models. *IEEE Trans Biomed Eng* 42: 304–312, 1995.
29. **Mari A, Gastaldelli A, Muscelli E, Natali A, Ferrannini E.** Relationships between glucose clearance during an OGTT and a euglycemic clamp. *Diabetes* 59: A377, 2010.
30. **Mari A, Stojanovska L, Proietto J, Thorburn AW.** A circulatory model for calculating non-steady-state glucose fluxes. Validation and comparison with compartmental models. *Comput Methods Programs Biomed* 71: 269–281, 2003.
31. **Mari A, Tura A, Gastaldelli A, Ferrannini E.** Assessing insulin secretion by modeling in multiple-meal tests. *Diabetes* 51: S221–S226, 2002.
32. **McGuinness OP, Mari A.** Assessment of insulin action on glucose uptake and production during a euglycemic-hyperinsulinemic clamp in dog: aA new kinetic analysis. *Metabolism* 46: 1116–1127, 1997.
33. **Meneilly GS, Elahi D, Minaker KL, Sclater AL, Rowe JW.** Impairment of noninsulin-mediated glucose disposal in the elderly. *J Clin Endocrinol Metab* 68: 566–571, 1989.
34. **Natali A, Gastaldelli A, Camastra S, Sironi AM, Toschi E, Masoni A, Ferrannini E, Mari A.** Dose-response characteristics of insulin action on glucose metabolism: a non-steady-state approach. *Am J Physiol Endocrinol Metab* 278: E794–E801, 2000.
35. **Nosadini R, Cipollina MR, Solini A, Sambataro M, Morocutti A, Doria A, Fioretto P, Brocco E, Muollo B, Frigato F.** Close relationship between microalbuminuria and insulin resistance in essential hypertension and non-insulin dependent diabetes mellitus. *J Am Soc Nephrol* 3: S56–S63, 1992.
36. **Del Prato S, Matsuda M, Simonson DC, Groop LC, Sheehan P, Leonetti F, Bonadonna RC, DeFronzo RA.** Studies on the mass action effect of glucose in NIDDM and IDDM: evidence for glucose resistance. *Diabetologia* 40: 687–697, 1997.
37. **Rizza RA, Mandarino LJ, Gerich JE.** Dose-response characteristics for effects of insulin on production and utilization of glucose in man. *Am J Physiol Endocrinol Metab* 240: E630–E639, 1981.
38. **Roden M, Krssak M, Stingl H, Gruber S, Hofer A, Fürnsinn C, Moser E, Waldhäusl W.** Rapid impairment of skeletal muscle glucose transport/phosphorylation by free fatty acids in humans. *Diabetes* 48: 358–364, 1999.
39. **Stingl H, Krssák M, Krebs M, Bischof MG, Nowotny P, Fürnsinn C, Shulman GI, Waldhäusl W, Roden M.** Lipid-dependent control of hepatic glycogen stores in healthy humans. *Diabetologia* 44: 48–54, 2001.
40. **Thiebaud D, Jacot E, Defronzo RA, Maeder E, Jequier E, Felber JP.** The effect of graded doses of insulin on total glucose uptake, glucose oxidation, and glucose storage in man. *Diabetes* 31: 957–963, 1982.
41. **Toschi E, Camastra S, Sironi AM, Masoni A, Gastaldelli A, Mari A, Ferrannini E, Natali A.** Effect of acute hyperglycemia on insulin secretion in humans. *Diabetes* 51: S130–S133, 2002.
42. **Tura A, Pacini G, Kautzky-Willer A, Gastaldelli A, DeFronzo RA, Ferrannini E, Mari A.** Estimation of prehepatic insulin secretion: comparison between standardized C-peptide and insulin kinetic models. *Metabolism* 61: 434–443, 2012.
43. **Uldry M, Ibberson M, Hosokawa M, Thorens B.** GLUT2 is a high affinity glucosamine transporter. *FEBS Lett* 524: 199–203, 2002.
44. **Yki-Järvinen H, Young AA, Lamkin C, Foley JE.** Kinetics of glucose disposal in whole body and across the forearm in man. *J Clin Invest* 79: 1713, 1987.
45. **Zhao FQ, Keating AF.** Functional Properties and Genomics of Glucose Transporters. *Curr Genomics* 8: 113–128, 2007.